Dynamic Chemical Devices: Generation of Reversible Extension/Contraction Molecular Motion by Ion-Triggered Single/Double Helix Interconversion

Mihail Barboiu,[a, b] Gavin Vaughan,[c] Nathalie Kyritsakas,[d] and Jean-Marie Lehn*[a]

Abstract: The polyheterocyclic strands **1-H** and **2-H** adopt a helical shape enforced by the pyridine–pyrimidine helicity codon. The crystal structure of **2-H** shows the formation of stacks of dimers of right- and left-handed individual helices. Treatment of **1-H** and **2-H** with silver triflate results in the generation of double-helical entities **1-DH** and **2-DH**, containing two strands and two silver ions. NMR studies and determination of the crystal structure of **2-DH** indicate that the duplex is stabilized by coordination of each Ag^+ ion to two terminal bipyridine units, one from each strand, and by pronounced $\pi-\pi$ stacking interactions between the internal heterocycles of the strands, yielding a very robust double helical structure. Reversible interconversion of the single and double helix may be achieved by addition of a cryptand capable of sequestering Ag^+ and releasing it by protonation. Thus, successive addition of acid and base leads to reversible interconversion between the shorter ($\sim$3.6 Å) single helix and the longer ($\sim$10.3 Å) double helix, resulting in the generation of pronounced extension/contraction motion. The system **1,2-H**/**1,2-DH** represents a dynamic chemical device undergoing ionic modulation of reversible molecular mechanical motion fueled by acid/base neutralization.

Keywords: helical structures · heterocyclic ligands · molecular dynamics · silver · supramolecular chemistry

Introduction

Controlled mechanical movement in molecular scale devices occurs in a variety of natural and artificial systems. Examples include nanomechanical switching processes involving conformational modifications triggered by changes in redox state or in temperature, by reversible binding of small molecules and ions, or by irradiation.[1–5] For instance rotary,[1, 2] linear,[4] and coiling/uncoiling[5] motions, induced by electrochemical or ionic reactions, have been achieved recently.

The interconversion of single and double helices produces specific molecular motions. The single/double-helix-type structural modifications play a most important role in biology, for instance in DNA double-strand breaks and repairing, in the course of the DNA replication process,[6] or in the formation of the gramicidin A dimer, as a cation selective channel across lipid bilayers.[7] Protein-[8] and DNA-based[9, 10] biomolecular motions involving single/double-helix conformational interconversions have been developed as dynamic nanoscaled devices. Some synthetic molecular strands[11, 12] and polymers[13] present double molecular winding induced by noncovalent interactions or by direct interstrand complementarity, as shown for oligopyridine-carboxamides in previous work from our laboratory.[12] Their dynamic exchange between simple and double molecular helices may be induced by solvent or temperature variations.

Of special interest is ionic modulation, that is, shape changes produced by ion binding, in particular in view of its relation to ion-induced processes in biology. As part of our studies on dynamic chemical devices,[5] we describe herein the ionic modulation of extension/contraction motions in a novel type of process involving the reversible switching between a molecular helical coil (**H**) and a metallosupramolecular double helix (**DH**), triggered by ion complexation–decomplexation reactions. The process is schematically depicted in Figure 1a.

It has recently been shown in our group that oligoheterocyclic strands such as **1-H** and **2-H**, consisting of alternating pyridine (py) and pyrimidine (pym) subunits connected in α,α' positions, fold into helical superstructures. In view of the

[a] Prof. J.-M. Lehn, Dr. M. Barboiu
Laboratoire de Chimie Supramoléculaire, ISIS
Université Louis Pasteur, CNRS UMR 7006
4 rue Blaise Pascal, 67000 Strasbourg (France)
Fax: (+33) 390-24-11-17
E-mail: lehn@chimie.u-strasbg.fr

[b] Dr. M. Barboiu
Present adress: Institut Européen des Membranes
CNRS UMR 5635, IEM/UMII, Place Eugène Bataillon
CC 047, 34095 Montpellier (France)

[c] Dr. G. Vaughan
European Synchrotron Radiation Facility
ESRF, BP 220, 38043, Grenoble Cedex (France)

[d] N. Kyritsakas
Laboratoire de Cristallochimie
Institut Le Bel, Université Louis Pasteur
4 rue Blaise Pascal, 67000 Strasbourg (France)

  0947-6539/03/0903-0763 $ 20.00+.50/0

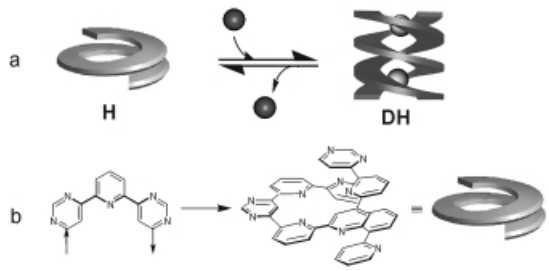

Figure 1. Concept and design of an ion-triggered molecular device. a) Ionic modulation of extension/contraction motions interconverting the molecular helical free ligand **H** and the metallosupramolecular double-helical dinuclear complex **DH**. b) Preferential *transoid*,*transoid* conformation leading to helical winding of extended pyridine–pyrimidine sequences.

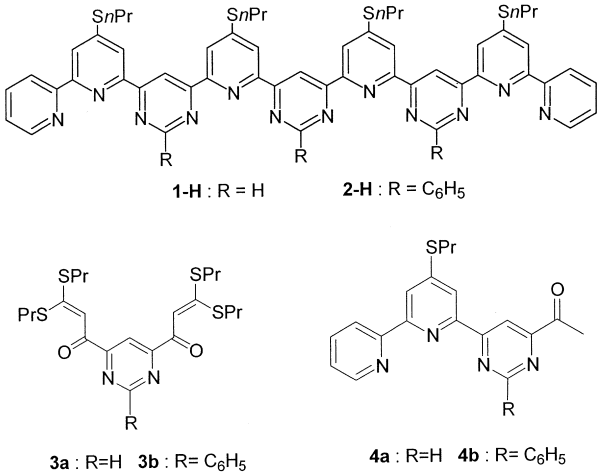

strongly favored *transoid* conformation about the connecting NC–CN bond in α,α'-bipyridine (bipy), α,α'-(py,pym) units are expected to have a similar or even stronger preference for the *transoid* form, so that α,α'-linked, extended (py–pym) sequences strongly enforce helical winding of the strand (Figure 1b).[14–16] Compounds **1-H** and **2-H** were synthesized by using Potts' methodology[17] following the strategy developed earlier:[15, 16] repetitive twofold reaction of the bifunctional central pyrimidine bis-Michael acceptor units **3a**,**b**[15, 18] with two methyl ketone building blocks **4a**,**b**[15, 18] yield **1-H** (34%) and **2-H** (54%), respectively. Compound **1-H** has been obtained earlier in the course of other work.[19]

A solution of **1-H** or **2-H** in $CDCl_3$ gives a sharp ^1H NMR spectrum consistent with the presence of a helical conformation of the polyheterocylic strands. As expected, on the basis of previous results,[15, 16] a strong shielding is observed for the terminal pyridine hydrogens H2 and H3 at $\delta = 6.66$ and 6.91 pm (**1-H**) and at $\delta = 6.58$ and 6.72 ppm (**2-H**), respectively (for numeration of the hydrogens, see Experimental Section). Moreover, distinct NOE effects are found between the protons oriented towards the interior of the helix, for example, between H3, H7, and H11 for **1-H** and between H3, H7, and H10 for **2-H**. The helical superstructure of compound **2-H** in solution was further confirmed by intermolecular NOESY interactions between the H_{ortho} protons of the two different phenyl rings grafted on internal and external pyrimidines. On the basis of these NMR data one may conclude that the molecular strands **1-H** and **2-H** adopt a helical conformation of about 1.5 turns in solution. Furthermore, a shielding displacement of 0.1 ppm was observed for the H2 and H3 protons of the terminal pyridines in a concentration range of 0.1–10 mM at 25 °C; in line with the X-ray crystal structure (see below), this effect agrees with the aggregation of compound **2-H** and corresponds to a dimerization constant K_{dim} of 255 ± 10 L mol^{-1} in $CDCl_3$ at 25 °C.

Abstract in French: *Les chaînes polyhétérocycliques **1-H** et **2-H** adoptent une structure hélicoïdale induite par le codon d'hélicité (pyridine–pyrimidine). La structure cristalline de **2-H** montre la formation de piles de dimères d'hélices individuelles droites et gauches. Le traitement de **1-H** et de **2-H** par le triflate d'argent conduit à la formation des entités en double hélice **1-DH** et **2-DH** contenant deux chaînes et deux ions argent. Des études par RMN et la détermination de la structure cristalline de **2-DH** montrent que le duplex est stabilisé par coordination de chaque Ag^+ à deux bipyridine terminales, appartenant chacune à l'un des brins, et par des interactions d'empilement entre les unités hétérocycliques internes des deux brins, formant ainsi une structure en double hélice très robuste. L'interconversion réversible entre l'hélice simple et la double hélice peut être réalisée par addition d'un cryptand capable de complexer Ag^+ et de le relibérer par protonation. Ainsi, des additions successives d'acide et de base conduisent à l'interconversion réversible entre une structure en hélice simple courte (~3.6 Å) et une structure en double hélice beaucoup plus longue (~10.3 Å), produisant un mouvement d'extension/contraction prononcé. Le système **1,2-H/1,2-DH** représente un dispositif chimique dynamique présentant une modulation ionique d'un mouvement mécanique moléculaire dont l'énergie est fournie par réaction de neutralisation acide/base.*

Crystal structure of the strand 2-H: Crystals of **2-H** suitable for X-ray structure determination were obtained by slow diffusion of acetonitrile into a solution of **2-H** in chloroform at room temperature. The molecular structure and packing are presented in Figure 2. The unit cell contains four **2-H** molecules of helical shape in two enantiomeric forms. The helix possesses a helical pitch of 3.62 Å and an interior void of about 1.93 Å diameter (considering a projection in a plane and taking into account the van der Waals radii of diagonally located N and C–H sites). This indicates a tight contact between the py–PrSpy–pym terminal aromatic rings, suggesting that $\pi-\pi$ and C–H$\cdots\pi$ (with an offset stacking angle[20] of about 19.5°) interactions play a role in the cohesion of the structure. The py–py torsional angles lie within about $11.8 \pm 1°$. The formation of the helix imposes a slight deviation from preferred planar conformation and the resulting py–pym torsional angle depends on whether the rings have central ($17.8 \pm 2°$) or terminal ($3.4 \pm 2°$) positions. The relative arrangement of the phenyl-substituted helices **2-H** in the crystal is different from previously reported helical-channel-type superstructures[16, 21] and deserves some comment. As

0947-6539/03/0903-0764 $ 20.00+.50/0 *Chem. Eur. J.* **2003**, *9*, No. 3

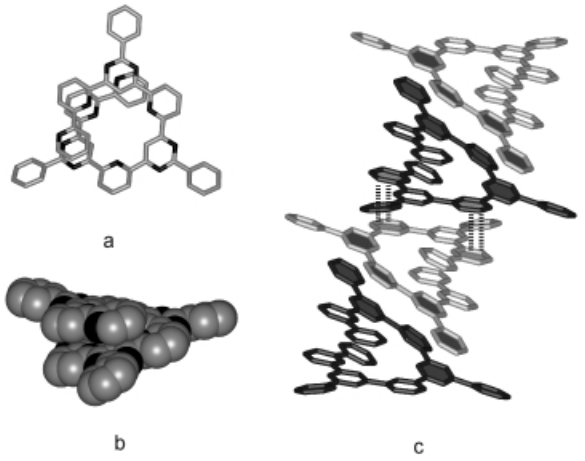

Figure 2. Crystal structure of helical free ligand **2-H**: a) stick representation; b) space-filing representation; c) representation of the packing of dimers of the right- and left-handed individual helices. The *n*PrS substituents have been omitted for clarity.

shown in Figure 2c, the right- and left-handed individual helices are $\pi-\pi$ stacked in dimeric aggregates (first/second and third/fourth molecules in Figure 2c, with a center of symmetry inside each dimer) presenting four intradimer aromatic ring overlaps: two between the internal pyrimidine and the phenyl rings grafted on the external pyrimidines (centroid–centroid distance of about 3.89 Å; offset stacking angle of about 20.2°) and two between the external pyrimidine and the internal PrS pyridines (centroid–centroid distance of about 4.07 Å; offset stacking angle of about 19.7°). The dimers interact by two intradimer aromatic ring overlaps between the internal and external PrS pyridines of strands with different handiness (centroid–centroid distance of about 4.5 Å; offset stacking angle of about 19.3°). Accordingly columnar arrays of $\pi-\pi$ stacked racemic helical dimers are generated in the solid state and in the solution from achiral strands **2-H** by the self-organization process.

Complexation of Ag^+ and formation of a metallo double helix by 1-H and 2-H: Initial complexation studies revealed that the addition of AgTf ($Tf = CF_3SO_3^-$) to acetonitrile suspensions of **1-H** or **2-H** caused a rapid dissolution of the ligand over **1-H**, **2-H**/Ag^+ stoichiometric ratio from 1:1 to 1:10. A ^1H NMR titration was therefore performed on solutions of AgTf and **1-H** and **2-H** in [D_3]acetonitrile. Below a **1-H**, **2-H**/Ag^+ ratio of 1:1, a very complex spectrum was obtained indicative of the presence of many slowly exchanging species in solution. At **1-H**, **2-H**/$Ag^+ = 1{:}1$ stoichiometry, a dramatic simplification of the spectrum was observed. The spectra consisted of a series of peaks that could be interpreted as ligands **1-H** or **2-H** in one magnetic environment and indicated high symmetry. Further incremental increases in the **1-H**, **2-H**/Ag^+ ratio up to 1:10 or concentrating a solution of silver complexes **1**-Ag^+ and **2**-Ag^+ did not modify the ^1H NMR spectra. Variable temperature measurements from $-50\,^\circ C$ to $+60\,^\circ C$ on **1**-Ag^+ led to only minor changes in proton chemical shift positions and no further apparent alteration in the species distributions. The ^{108}Ag NMR spectra of **1**-Ag^+ and **2**-Ag^+ showed only one signal at $\delta = 444.2$ and 427.3 ppm, respectively. The two-dimensional $^1H-^{108}Ag$ NMR correlation spectra provided decisive information, indicating a precise localization of the silver ions on the two terminal bipyridine groups. The electrospray mass spectra of the **1**-Ag^+ and **2**-Ag^+ complexes showed peaks indicating dimeric species at m/z 1104 for $[Ag_2(\mathbf{1\text{-}H})_2]^{2+}$ and 1132 $[Ag_2(\mathbf{2\text{-}H})_2]^{2+}$. The charge state of these ions were determined by isotopic profile simulations, which corresponded to symmetrical profiles of the doubly charged dimeric cations.

The ^1H NMR spectra of **1-**Ag^+ and **2-**Ag^+ showed a deshielding of the protons H2 and H3 of the terminal pyridines ($\delta = 6.92$ and 7.56 and $\delta = 7.03$ and 7.19 ppm respectively) due to the silver ion complexation. The other signals were overall strongly shielded ($\Delta\delta = 1.5$ ppm) with respect to the monomeric species **1-H** and **2-H** (see Figure 4b below), suggesting that intermolecular $\pi-\pi$ stacking interactions played an important role in the aggregation process of these compounds.

Furthermore, numerous correlation signals due to strong $\pi-\pi$ stacking interactions were observed in the ROESY spectra of **1**-Ag^+ and **2**-Ag^+. Distinct NOE effects between the protons H4 of terminal pyridines and the protons H5 of the external PrS-pyridines, indicated an orthogonal complexation of silver ions by two terminal bipyridines. Moreover, NOE interactions were observed between the protons H_7 and H_{11}, H_8 and H_{12} for **1-DH** as well as between H_7 and H_{10} for **2-DH**. These protons are also correlated with both internal and external PrS-pyridine protons.

Anticipating the crystal structure results below, all these NMR spectroscopic data agree with the formulation of the silver complexes **1**-Ag^+ and **2**-Ag^+ of the molecular strands **1-H** and **2-H** in acetonitrile, as double helical structures **1-DH** and **2-DH**: two intertwined monomeric strands stacked all along their length generate a double helical superstructure induced and stabilized by silver ion complexation at the terminal bipyridine moieties. This double helical structure is highly robust, since it is still the only compound observable even in presence of a very large excess of silver ions (up to 1:10 ligand/ion ratio) and despite the presence of several unoccupied ion binding sites. The same is indicated by the conservation of an unchanged proton NMR spectrum for **1-DH** at $+60\,^\circ C$.

Crystal structure of the double-stranded complex 2-DH: The crystal structure of the complex of **2-H** with Ag^+ was determined on crystals obtained from a solution of the complex in acetonitrile/isopropyl ether (1:1) at room temperature (Figure 3). The unit cell was found to contain four double-helical complexes **2-DH**, two of each helical sense stacked on each other, together

The two intertwined monomeric strands are held in double-helix form by two silver cations bound to the terminal bipy units and presenting a partially flattened tetrahedral coordination geometry. Preferential complexation at the bipy sites is in line with the stronger binding to the pair of more basic py nitrogens, as compared to internal (py, pym) units containing a less basic pym nitrogen. The averaged Ag–N bond lengths in **2-DH**, Ag–py_1 (2.24 Å) and Ag–$PrSpy_2$ (2.40 Å) are similar to those found in the silver helicates.[22] The two intertwined

  0947-6539/03/0903-0765 $ 20.00+.50/0

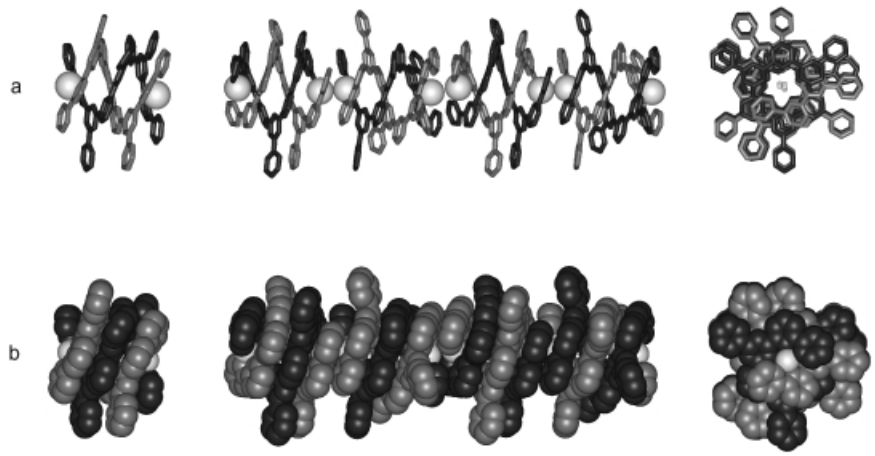

Figure 3. Crystal structure of the double-helical silver complex **2-DH** (left) and of the arrangement of the **2-DH** entities in the crystal (center and right): a) stick representation; b) space-filling representation. In the stick view along the axis of the stacks (top right), the silver ions are shown in reduced size. The *n*PrS substituents have been omitted for clarity.

ligands of **2-DH** form a 1.5 turn duplex with a helical pitch of about 6.9 Å, corresponding to average py–pym torsional angles of 26.1° (15.7–31.7°), significantly opened up with respect to those in the single-helical structure **2-H**. The **2-DH** entity is reminiscent of the double-stranded multinuclear Cu^+ and Ag^+ helicates described earlier.[3, 22–24]

As expected from the solution studies, the double-helix structure allows considerable overlap between the aromatic groups of each monomeric strand with an average π–π-stacking centroid–centroid distance of 3.56 Å corresponding to van der Waals contact. In contrast to the single-helical structure of **2-H**, in which aromatic rings are slightly slipped, in the double helix **2-DH** aromatic rings are situated in face-to-face stacking arrangement. They are stabilized by favorable dipole–dipole (Scheme 1, A, B) or dipole–complexation-induced-dipole (Scheme 1 C, D, E) electrostatic interactions between π-donor and π-accepting nitrogen-containing ring systems; these generate a double helical structure composed of four π–π stacking subsets, that is, two pairs of four and of three overlapping aromatic rings.

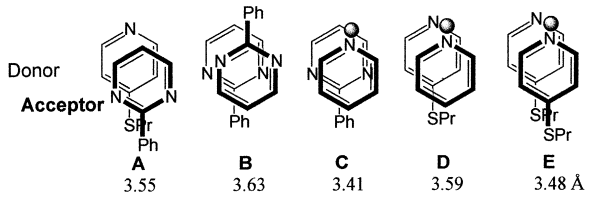

Scheme 1. Types of donor–acceptor π–π stacking interactions observed in the crystal stucture of **2-DH** and measured centroid–centroid distances.

Thus, the robustness of the double helical superstructure results from the compatibility and the synergistic effect of the metal ion binding at the termini of the strands and of the large stacking interaction between the two strands. The latter is due to a molecular recognition type complementary positioning of the stacked heterocyclic units. One may point out that the role of the stacking interactions in the present duplex structures is related to that in the previously described helicates[22–24] and artificial double helices,[12] as well as to the significant contribution of stacking to the stabilization of the double-helical structure of nucleic acids.[25] The role of silver ions in the formation of the **2-DH** duplex also bears relation to the stabilization of a DNA duplex, containing an alternative base pair of pyridine nucleobases, by coordination with Ag^+ ions.[26]

The structure of **2-DH** is highly regular and may be propagated in one direction without any structural modification. In the crystal, each duplex of one helical sense is π–π stacked with two duplexes of the same helical sense (Figure 3). These π–π stacking interactions involve the terminal (acceptor) pyridine and the external (donor) PrS-pyridine both complexed by silver ions and stacked on each other in a opposite way. Each $[Ag_2(\mathbf{2\text{-}H})_2]$ double-helix entity presents a tight contact with the two neighboring ones by stacking of the respective terminal bipys (centroid–centroid distance of about 3.63 Å; offset stacking angle of about 18°). This pattern generates infinite double-helix stacks of **2-DH** units of one helical sense. Accordingly, chiral double helical channels are generated in the solid state with an interior void of about 1.8 Å (considering a projection in a plane and taking into account the van der Waals radii of diagonally located N and C–H sites). The silver ions are arranged into an approximately linear array tightly fitting into the central cavity of the double helical channel.

Ionic modulation of single helix/double helix interconversion with extension/contraction motion: We have recently shown that the contraction/extension motions, generated by the interconversion between a helical ligand strand and its extended linear complex, could be chemically controlled in a manner reminiscent of that of proteins capable of transforming physicochemical modifications into motion.[5] This system represents a prototype for a molecular actuator/engine type of dynamic device "fueled" by ionic processes.

The transformation of the helical free ligands **1-H**, **2-H** into the corresponding robust double-helical silver complexes **1-DH** and **2-DH** offers the unique opportunity to set up a reversible motion process in which a molecular entity undergoes sequential extension and contraction phases upon single/double helix interconversion, triggered by external chemical effectors. A system that produced reversible pulses of Ag^+ ions was achieved by taking advantage of the properties of the macrobicyclic ligand cryptand [2.2.2],[27], which forms cryptate inclusion complexes $[M^{n+} \subset 2.2.2]$ with numerous metal ions.[27]

Figure 4b shows the evolution of the aromatic and aliphatic parts of the ^1H NMR spectra as a function of a triggering agent: Ag^+, [2.2.2], CF_3SO_3H, or LiOH.

0947-6539/03/0903-0766 $ 20.00+.50/0 *Chem. Eur. J.* **2003**, *9*, No. 3

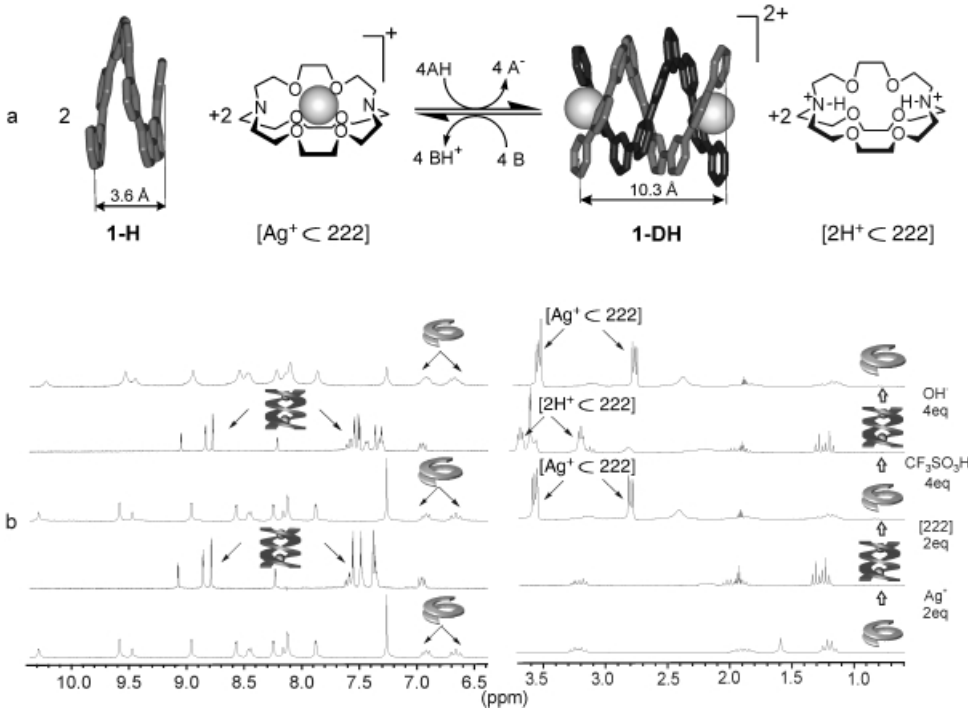

Figure 4. a) Ionic modulation of reversible extension/contraction motional process upon single/double helix interconversion between **1-H** and **1-DH**. b) 500 MHz ^{1}H spectral changes on structural interconversion in the system **1-H**/**1-DH** on successive addition of the different triggering agents (see text). The values of 3.6 and 10.3 Å indicated for **1-H** and **1-DH**, respectively, correspond to distances between carbon centers. The gray spherical objects represent Ag^+ ions; AH = CF_3SO_3H ; B = LiOH. The *n*PrS substituents have been omitted for clarity.

The addition of one equivalent of Ag^+ to a solution ($CDCl_3$/CD_3CN = 2/1 v/v) of helical ligand **1-H** leads to the double helical complex **1-DH**. This transformation is characterized by the disappearance of the shielded signals of the terminal pyridine hydrogens H2 and H3 and by the appearance of deshielded signals of the Ag^+ complexed pyridine, as well as by the marked shielding of π–π stacked pyrimidine and PrS-pyridine hydrogen atom. On addition of a strong Ag^+ complexant such as the [2.2.2] cryptand, the shielded signals of the helical form **1-H** reappear and the aliphatic part of the spectrum shows peaks that correspond to the cryptate inclusion complex [Ag^+ ⊂ 2.2.2]. Lowering the pH induces protonation of the bridgehead nitrogens of the cryptate causing the release of the complexed Ag^+ ions, which then bind to the monohelical form **1-H** leading to the double helical complex **1-DH**. The aliphatic part of the spectrum shows peaks that correspond to protonated cryptand [$2H^+$ ⊂ 2.2.2]. Subsequent deprotonation of the latter by addition of LiOH restores the spectrum of the monohelical form **1-H** and of the cryptate [Ag^+ ⊂ 2.2.2]. Single/double-helical interconversions of the helical entity **1-H** and the double helical complex **1-DH** can be pursued in this way by successive additions of acid and base, controlling the repetitive exchange of Ag^+ between the ligand **1-H** and the [2.2.2] cryptand. The interconversion is complete within the time of mixing and recording the NMR spectra. It may be expected to occur appreciably faster, since its rate is determined by the rate of protonation induced dissociation of the silver cryptate.[27]

Since the overall length of the single helix **1-H** is about 3.6 Å and that of the double helix **1-DH** is 10.3 Å, the **1-H**/**1-DH** interconversion generates a marked extension/contraction motion (Figure 4a). A related process takes place in the monomer–dimer interconversion of helically preorganized oligopyridine-dicarboxamide strands, in which the dynamic exchange is concentration, solvent, and temperature dependent.[12] One may also recall the electrochemically triggered interconversion between a double-stranded helicate and a single-stranded complex described early on.[28] In the present case, the modulation of the coupled single/double-helix extension/contraction structural-switching processes (Figure 5) is induced by coupled ion-binding/protonation events and fuelled by acid–base neutralization reactions.

Conclusion

The present results show that by using a rationally designed helical molecular strand and a simple chemical mechanism, it is possible to control, through ion binding, single/double-helix transformation-induced molecular motions reminiscent of stretching/contracting actions that occur during DNA replications[6] or in the formation of the gramicidin A dimer, as a cation selective channel across lipid bilayers.[7]

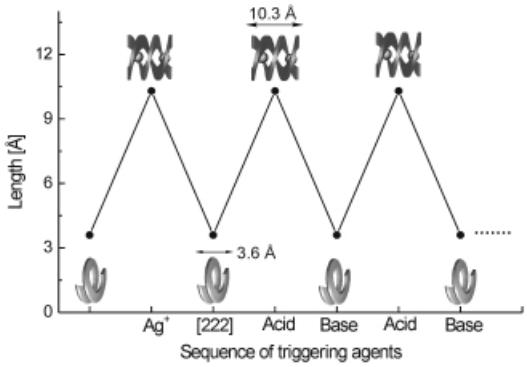

Figure 5. Iono-mechanical cycles generated by the modulation of the single/double-helix, compression/extension process **2-H** ⇌ **2-DH** by coupled ion/pH-induced structural switching.

The system described here represents a molecular actuator/engine type of dynamic device, displaying spring-like extension/compression motions, fuelled by ionic processes, and undergoing iono-mechanical cycles, amenable to perform mechanical work in a periodic manner.[5, 29] It achieves ion-triggered muscle-type extension-contraction through a mechanism different from both the biological one and that in other model systems.[1, 2, 4] The entities involved also provide a

framework for arranging peripheral residues (of interest in biology or materials science) into a robust double helical array and for modifying their relative location through twisting around the helical axis in the course of single/double-helix interconversion. Finally, they offer intriguing potential for the design of dynamic supramolecular devices displaying ionically triggered shape changes of interest for molecular information transfer.

Experimental Section

General methods: All reagents were obtained from commercial suppliers and used without further purification. THF was distilled over benzophenone/Na. All organic solutions were routinely dried by using sodium sulfate (Na_2SO_4). Column chromatography was carried out on Merck alumina activity II-III.

^{1}H NMR, ^{108}Ag NMR, and COSY, ROESY, and ^{1}H-^{108}Ag NMR correlation measurements were recorded on an ARX 500 MHz Bruker spectrometer in $CDCl_3$ and CD_3CN, with the use of the residual solvent peak as reference. Mass spectrometric studies were performed in the positive ion mode using a quadrupole mass spectrometer (Micromass, Platform II). Samples were dissolved in acetonitrile and were continuously introduced into the mass spectrometer at a flow rate of 10 mL min^{-1} through a Waters 616HPLC pump. The temperature (60 °C) and the extraction cone voltage ($V_c = 5$–10 V) were usually set to avoid fragmentations. The microanalyses were carried out at Service de Microanalyses, Institut Charles Sadron, Strasbourg.

The numeration used for the assignments of the 1H NMR signals (according to the corresponding COSY and ROESY spectra) are given below.

Synthesis of ligands and complexes: Compounds **3a**,**b** and **4a**,**b** were prepared according to the procedures described in the literature (**3a** and **4a**[15] **3b** and **4b**[18]).

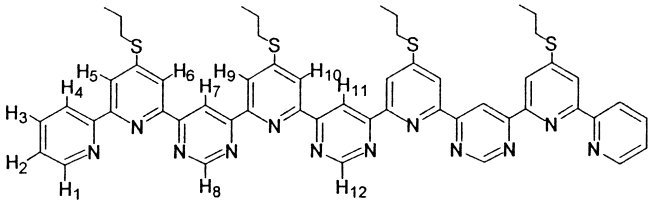

Compound 1-H: A solution of *t*BuOK (108 mg, 0.96 mmol) in dry THF (15 mL) was added under argon over a period of 2 h to a refluxing solution of **3a** (120 mg, 0.24 mmol), **4a** (170 mg, 0.48 mmol), and [18]crown-6 (128 mg, 0.48 mmol) in dry THF (20 mL). The solution was stirred overnight at room temperature, and acetic acid (1 mL) and NH_4OAc (1 g) were added to the reaction. The mixture was refluxed for 90 min, cooled, poured into water (100 mL) extracted with chloroform (3 × 100 mL), washed with saturated aqueous $NaHCO_3$ (100 mL), and dried with Na_2SO_4. After evaporation the crude material was purified by flash chromatography (alumina/chloroform) to give **1-H** (85 mg, 34 %). ^{1}H NMR ($CDCl_3$): $\delta = 10.28$ (s, 1H; H11), 9.58 (s, 2H; H7), 9.47 (s, 1H; H12), 8.96 (s, 2H; H8), 8.57 (d, $J = 1.2$ Hz, 2H; H10), 8.45 (dd, 2H; $J = 3.6$ Hz, H1), 8.25 (d, $J = 1.2$ Hz, 2H; H6), 8.16 (dd, $J = 7.6$ Hz, 2H; H4), 8.12 (d, $J = 1.2$ Hz, 2H; H9), 7.88 (d, $J = 1.2$ Hz, 2H; H5), 6.91 (dt, $J = 3.6$ Hz, 2H; H3), 6.66 (dt, $J = 7.6$ Hz, 2H; H2), 3.24 (t, $J = 7.9$ Hz, 8H), 1.88 (sext, $J = 7.9$ Hz, 8H), 1.21 ppm (t, $J = 7.9$ Hz, 12H); ^{13}C NMR ($CDCl_3$): $\delta = 13.85$, 13.93, 22.02, 22.24, 29.97, 33.10, 33.24, 114.16, 114.47, 117.47, 118.69, 119.74, 122.07, 123.50, 135.54, 146.32, 151.84, 152.11, 152.43, 153.44, 154.19, 158.32, 158.34, 162.44, 162.62, 162.72, 162.81 ppm; FAB-MS: *m*/*z* (%): 996.5 (100) $[M+H]^+$; elemental analysis calcd (%) for $C_{54}H_{50}N_{12}S_4$ (995.3): C 65.16, H 5.06, N 16.89; found: C 62.49, H 5.36, N 15.10.

Silver complex 1-DH: Formation from ligand **1-H** (5 mg), and AgOTf (1.3 mg) in CD_3CN (0.5 mL) at room temperature. ^{1}H NMR (CD_3CN): $\delta =$ 9.06 (s, 1H; H11), 8.83 (s, 2H; H7), 8.77 (s, 2H; H8), 8.20 (s, 1H; H12), 7.57 (dt, $J = 4.8$ Hz, 2H; H3), 7.54 (d, 2H; $J = 1.8$ Hz, H9), 7.47 (d, $J = 1.8$ Hz, 2H; H10), 7.46 (dd, $J = 7.7$ Hz, 2H; H1), 7.36 (d, $J = 1.8$ Hz, 2H; H6), 7.35 (dd, $J = 7.7$ Hz, 2H; H4), 7.34 (d, $J = 1.8$ Hz, 2H; H5), 6.94 (dt, $J = 4.8$ Hz, 2H; H2), 3.24 (t, $J = 7.9$ Hz, 4H), 3.18 (t, $J = 7.9$ Hz, 4H), 2.01 (sext, $J =$ 7.9 Hz, 4H), 1.93 (sext, $J = 7.9$ Hz, 4H), 1.30 (t, $J = 7.9$ Hz, 6H), 1.23 ppm (t, $J = 7.9$ Hz, 6H); ^{108}Ag NMR (CD_3CN): $\delta = 444.2$ ppm; ES-MS: *m*/*z* (%): 1104.5 (100) $[Ag_2(\mathbf{1\text{-}H})_2]^{2+}$; elemental analysis calcd (%) for $C_{110}H_{100}N_{24}S_{10}0_6F_6Ag_2$ (2504.5): C 52.75, H 4.02, N 13.42; found: C 52.49, H 4.33, N 14.10.

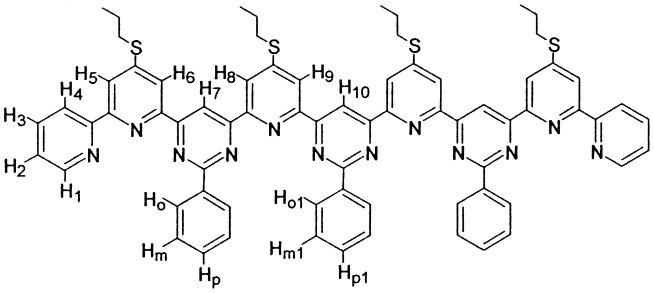

Compound 2-H: A solution of *t*BuOK (174 mg, 1.54 mmol) in dry THF (15 mL) was added under argon over a period of 2 h to a refluxing solution of **3b** (217 mg, 0.38 mmol), **4b** (330 mg, 0.78 mmol), and [18]crown-6 (205 mg, 0.78 mmol) in dry THF (20 mL). The solution was stirred overnight at room temperature, and acetic acid (1 mL) and NH_4OAc (1 g) were added to the reaction. The mixture was refluxed for 90 min, cooled, poured into water (100 mL) extracted with chloroform (3 × 100 mL), washed with saturated aqueous $NaHCO_3$ (100 mL), and dried with Na_2SO_4. After evaporation the crude material was purified by flash chromatography (alumina/chloroform) to give **2-H** (250 mg, 54 %). ^{1}H NMR ($CDCl_3$): $\delta = 9.89$ (s, 1H; H10), 9.24 (s, 2H; H7), 8.72 (m, 2H; H_{o1}), 8.44 (m, 4H; H_o), 8.20 (d, $J = 1.1$ Hz, 2H; H5), 8.17 (d, $J = 1.1$ Hz, 2H; H6), 8.15 (dd, 2H; $J = 7.6$ Hz, H4), 8.07 (dd, $J = 7.9$ Hz, 2H; H1), 7.96 (d, $J = 1.2$ Hz, 2H; H8), 7.89 (d, $J = 1.2$ Hz, 2H; H9), 7.63 (m, 3H; H_{m1} H_{p1}), 7.57 (m, 6H; H_m H_p), 6.72 (dt, $J = 7.6$ Hz, 2H; H3), 6.58 (dt, $J = 7.9$ Hz, 2H; H2), 3.17 (t, $J = 7.9$ Hz, 4H), 3.05 (t, $J = 7.9$ Hz, 4H), 1.90 (sext, $J = 7.9$ Hz, 8H), 1.25 ppm (dt, $J = 7.9$ Hz, 12H); ^{13}C NMR ($CDCl_3$): $\delta = 13.80$, 13.88, 22.04, 22.37, 32.84, 32.91, 114.26, 117.97, 118.07, 119.17, 121.12, 123.25, 128.40, 128.58, 130.38, 135.42, 147.88, 151.19, 152.44, 153.46, 153.98, 154.05, 154.38, 162.69, 163.17 ppm; FAB-MS: *m*/*z* (%): 1223.4 (100) $[M+H]^+$; elemental analysis calcd (%) for $C_{72}H_{62}N_{12}S_4$ (1222.4): C 70.64, H 5.11, N 13.74; found: C 70.72, H 5.36, N 13.44.

Silver complex 2-DH: Formation from ligand **2-H** (5 mg) and AgOTf (1.1 mg) in CD_3CN, (0.5 mL) at room temperature. ^{1}H NMR (CD_3CN): $\delta =$ 8.84 (s, 2H; H7), 8.40 (m, 2H; H_{o1}), 8.34 (m, 4H; H_o), 7.97 (s, 1H; H10), 7.94 (d, $J = 1.8$ Hz, 2H; H9), 7.68 (m, 3H; H_{m1} H_{p1}), 7.63 (d, $J = 1.8$ Hz, 2H; H8), 7.61 (d, $J = 1.5$ Hz, 2H; H6), 7.58 (m, 6H; H_m H_p), 7.45 (dd, $J = 7.6$ Hz, 2H; H1), 7.21 (dt, $J = 4.8$ Hz, 2H; H4), 7.20 (dt, $J = 4.8$ Hz, 2H; H3), 7.03 (d, $J =$ 1.5 Hz, 2H; H5), 6.69 (dt, $J = 7.6$ Hz, 2H; H2), 3.08 (m, 4H), 2.86 (m, 4H), 1.89 (sext, $J = 7.9$ Hz, 4H), 1.58 (sext, $J = 7.9$ Hz, 4H), 1.24 (t, $J = 7.9$ Hz, 6H), 0.97 ppm (t, $J = 7.9$ Hz, 6H); ^{108}Ag NMR (CD_3CN): $\delta = 427.3$; ES-MS: *m*/*z* (%): 1332.2 (100) $[Ag_2(\mathbf{2\text{-}H})_2]^{2+}$; elemental analysis calcd (%) for $C_{146}H_{124}N_{24}S_{10}0_6F_6Ag_2$ (2961.1): C 59.22, H 4.22, N 11.35; found: C 59.08, H 4.73, N 11.23.

X-ray crystallographic data for ligand 2-H and complex 2-DH: Single crystals of **2-H** $[4(C_{72}H_{62}N_{12}S_4)]$ were grown from acetonitrile/chloroform. Crystals were placed in oil and a single colorless crystal of dimension 0.20 × 0.20 × 0.16 mm was selected, mounted on a glass fiber, and placed in a low-temperature N_2 stream. The unit cell was monoclinic with a space group of $P2_1/c$. Cell dimensions: $a = 14.8045(3)$, $b = 16.3781(6)$, $c = 26.300(1)$ Å, $\alpha = \gamma = 90°$, $\beta = 91.232(5)°$, $V = 6375.5(4)$ Å^3, $Z = 4$ ($M_r = 2568$, $\rho = 1.27$ g cm^{-3}). Reflections were collected from $2.5 \le \theta \le 27.47°$ for a total of 13854, of which 6335 were unique with $I > 3\sigma(I)$; number of parameters = 793. Final *R* factors were $R_1 = 0.072$ (based on observed data), $wR_2 = 0.085$ (based on all data), GOF = 1.024, maximal residual electron density was 0.541 e Å^{-3}.

Single crystals of **2-DH** $[2(C_{144}H_{124}N_{24}Ag_2S_8)\cdot 4CF_3SO_3\cdot 2C_6H_{14}O]$ were grown from isopropyl ether/acetonitrile. Crystals were placed in oil, and a single colorless crystal of dimension 0.20 × 0.20 × 0.20 mm was selected,

0947-6539/03/0903-0768 $ 20.00+.50/0 *Chem. Eur. J.* **2003**, *9*, No. 3

mounted on a glass fiber, and placed in a low-temperature N_2 stream. The unit cell was triclinic with a space group of $P\bar{1}$. Cell dimensions: $a=17.8924(18)$, $b=25.003(2)$, $c=35.302(4)$ Å, $\alpha=105.347(5)^\circ$, $\beta=96.354(4)^\circ$, $\gamma=105.680(5)^\circ$, $V=14378(3)$ Å^3, $Z=4$ ($M_r=5936$, $\rho=1.333$ g cm^{-3}). Reflections were collected from $4.93\leq\theta\leq16.47^\circ$ for a total of 68552, of which 36807 were unique with $I>2\sigma(I)$; number of parameters = 3679. Final R factors were $R_1=0.0813$ (for $I/\sigma>4$), $wR_2=0.1125$ (based on all data), GOF = 1.027, maximal residual electron density was 1.605 e Å^{-3}. Rwp was 0.208 for $I/\sigma>4$, and 0.228 for all data.

X-ray diffraction data for **2-H** were collected on a Nonius Kappa charge-coupled device (CCD) diffractometer with a graphite monochromatized $Mo_{K\alpha}$ radiation ($\lambda=0.71073$ Å). ϕ scans at 173, at the Laboratoire de Cristallochimie, Université Louis Pasteur, Strasbourg. X-ray diffraction data measurements for **2-DH** were carried out at beamline ID11 at the European Synchrotron Facility (ESRF) at Grenoble. A wavelength of 0.51593 Å was selected by using a double crystal Si (111) monochromator, and data were collected using a Bruker "Smart" CDD camera system at fixed 2θ. Data were reduced by using the Bruker SAINT software. The structures of **2-H** and **2-DH** were determined by using direct methods and refined (based on F^2 with all independent data) by full-matrix least-square methods (SHELXTL 97). Hydrogen atoms were included at calculated positions by using a riding model.

CCDC-195295 (**2-H**), and CCDC-195419 (**2-DH**) contain(s) the supplementary crystallographic data for this paper. These data can be obtained free of charge via www.ccdc.cam.ac.uk/conts/retrieving.html (or from the Cambridge Crystallographic Data Centre, 12 Union Road, Cambridge CB21EZ, UK; fax: (+44) 1223-336-033; or e-mail: deposit@ccdc.cam.ac.uk).

Acknowledgement

We thank Dr. Roland Graff for NMR measurements. This research was supported by the CNRS and the Collège de France (post-doctoral fellowship to M.B.).

[1] *Acc. Chem. Res.* **2001**, *34*, special issue on molecular machines.
[2] V. Balzani, F. Credi, M. Raymo, J. F. Stoddart, *Angew. Chem.* **2000**, *112*, 3486–3531; *Angew. Chem. Int. Ed.* **2000**, *39*, 3348–3391.
[3] J.-M. Lehn, *Supramolecular Chemistry-Concepts and Perspectives*, VCH, Weinheim, **1995**, pp. 124–138.
[4] J.-P. Collin, C. Dietrich-Buchecker, P. Gavina, M. C. Jimenez-Molero, J.-P. Sauvage, *Acc. Chem. Res.* **2001**, *34*, 477–487.
[5] M. Barboiu, J.-M. Lehn, *Proc. Natl. Acad. Sci.* **2002**, *99*, 5201–5206.
[6] K.-M. Chou, Y.-C. Cheng, *Nature* **2002**, *415*, 655–659.
[7] D.A Langs, *Science* **1988**, *241*, 188–191.
[8] F. J. Nédélec, T. Surrey, A. C. Maggs, S. Leiber, *Nature* **1997**, *389*, 305–308.
[9] C. Mao, W. Sun, Z. Shen, N. C. Seeman, *Nature* **1999**, *397*, 144–146.
[10] B. Yurke, A. J. Tuberfield, A. P. Mills Jr., F. C. Simmel, J. L. Neumann, *Nature* **2000**, *406*, 605–608.
[11] D. J. Hill, M. J Mio, R. B. Prince, T. S. Hughes, J. S. Moore, *Chem. Rev.* **2001**, *101*, 3893–4011.
[12] V. Berl, I. Huc, R. G. Khoury, M. J. Krische, J.-M. Lehn,. *Nature* **2000**, *407*, 720–723; V. Berl, I. Huc, R. G. Khoury, J.-M. Lehn, *Chem. Eur. J.* **2001**, *7*, 2798–2809;V. Berl, I. Huc, R. G. Khoury, J.-M. Lehn, *Chem. Eur. J.* **2001**, *7*, 2810–2820.
[13] T. Nakano, Y. Okamoto, *Chem. Rev.* **2001**, *101*, 4013–4038.
[14] G. S. Hannan, J.-M. Lehn, N. Kyritsakas, J. Fischer, *J. Chem. Soc. Chem. Commun*. **1995**, 765–766.
[15] D. M. Bassani, J.-M. Lehn, G. Baum, D. Fenske, *Angew. Chem.* **1997**, *109*, 1931–1933; *Angew. Chem. Int. Ed. Engl*. **1997**, *36*, 1845–1847; D. M. Bassani, J.-M. Lehn, *Bull. Soc. Chim. Fr.* **1997**, *134*, 897–906.
[16] M. Ohkita, J.-M. Lehn, G. Baum, D. Fenske, *Chem. Eur. J.* **1999**, *12*, 3471–3481.
[17] K. T. Potts, K. A Gheysen-Raiford,. M. Keshavarz-K, *J. Am.Chem. Soc.* **1993**, 115, 2793–2807.
[18] K. M. Gardinier, R. G. Khoury, J.-M. Lehn, *Chem. Eur. J.* **2000**, *6*, 4124–4131.
[19] A. M. Garcia, F. J. Romero-Salguero, D. M. Bassani, J.-M. Lehn, G. Baum, D. Fenske, *Chem. Eur. J.* **1999**, *5*, 1803.
[20] C. Janiak, *J. Chem. Soc. Dalton Trans.* **2000**, 3885–3896.
[21] L. A. Cuccia, J.-M. Lehn, J.-C. Homo, M. Schmutz, *Angew. Chem.* **2000**, *112*, 239–243; *Angew. Chem. Int. Ed.* **2000**, *39*, 233–237.
[22] T. M. Garrett, U. Koert, J.-M. lehn, A. Rigault, D. Meyer, J. Fischer, *J. Chem. Soc. Chem. Commun*. **1990**, 557; C. Provent, S. Hewage, G. Grand, G. Bernardinelli, L. J. Charbonnière, A. F. Williams, *Angew. Chem.* **1997**, *109*, 1346–1348; *Angew. Chem. Int. Ed. Engl*. **1997**, *36*, 1287–1289.
[23] J.-M. Lehn, A. Rigault, J. Siegel, J. Harrowfield, B. Chevrier, D. Moras, *Proc. Natl. Acad. Sci. USA* **1987**, *84*, 2565.
[24] J.-M. Lehn, A. Rigault, *Angew. Chem.* **1988**, *100*, 1121–1122; *Angew. Chem. Int. Ed. Engl.* **1988**, *27*, 1095–1097.
[25] E. T. Kool, J. C. Morales, K. M. Guckian, *Angew. Chem.* **2000**, *112*, 1046–1068; *Angew. Chem. Int. Ed*. **2000**, *39*, 990–1009; P. Hobza, J. Sponer, *J. Am. Chem. Soc.* **2002**, *124*, 11802–11 808.
[26] K. Tanaka, Y. Yamada, M. Shionoya, *J. Am. Chem. Soc.* **2002**, *124*, 8802–8803.
[27] J.-M. Lehn, *Struct. Bonding* **1973**, *16*, 1–69; J.-M. Lehn, J.-P. Sauvage, *J. Am. Chem. Soc.* **1975**, *97*, 6700–6707; J.-M. Lehn, *Acc. Chem. Res.* **1978**, *11*, 49–57.
[28] J.-P. Gisselbrecht, M. Gross, J.-M. Lehn, J.-P. Sauvage, R. Ziessel, C. Piccini-Leopardi, J.-M. Arrieta, G. Germain, M. Van Meerssche, *Nouv. J. Chim.* **1984**, *8*, 661–667; see also ref. [3] p. 132.
[29] For a recently described case of stretching/contraction optomechanical cycle, see: T. Hugel, N. B. Holland, A. Cattani, L. Moroder, M. Seitz, H. E. Gaub, *Science* **2002**, *296*, 1103–1106.

Received: September 3, 2002 [F4387]

  0947-6539/03/0903-0769 $ 20.00+.50/0